Exact solution for the density of electronic states in a model of a disordered system

M. V. Sadovskiĭ

Institute of the Physics of Metals, Ural Scientific Center, Academy of Sciences of the USSR
(Submitted 24 May 1979)
Zh. Eksp. Teor. Fiz. **77**, 2070–2080 (November 1979)

A one-dimensional system of electrons is considered, in a Gaussian random field with a correlator whose form (in the momentum representation) is a Lorentzian with its center at $Q = 2p_F$. This can be considered as a Gaussian model of the Peierls transition in the fluctuation region. An exact summation of all Feynman diagrams is carried out, and a representation of the averaged one-electron Green's function as a continued fraction is obtained. A density of states with a characteristic pseudogap is found. It is shown that when the correlation range of the short-range order is decreased there is a gradual filling in of the pseudogap and a transition to a "metallic" state.

PACS numbers: 71.20. + c, 71.30. + h, 71.25.Cx

INTRODUCTION

There is a limited number of models of the electronic structure of one-dimensional disordered systems that admit of exact solution.[1] Interest in such models is due both to the general problem of studying the electronic properties of disordered systems and to questions of the physics of quasi-one-dimensional systems, the majority of which display some sort or other of properties associated with their disorder. In the last few years several important new results have been obtained, casting considerable light on the situation of an electron in a one-dimensional random field.[2-4] This work is also mostly characterized by the use of specific methods of solution, specially adapted to the solution of one-dimensional problems, and as a rule not capable of further generalization because they are so cumbersome. Only in a very few cases is it possible to obtain an exact solution of a problem about the electron in a one-dimensional random field by means of standard methods of present-day many-particle theory.[5]

One model of this sort was proposed some time ago by the present writer (see Ref. 6). In the framework of this model it could be shown now the scattering of the electron by a random field with a definite type of short-range order leads to the formation of a peculiar "band structure" of the energy spectrum, which appears in the form of a characteristic pseudogap in the density of electronic states, in the absence of any sort of long-range order. It was also possible to consider high-frequency conductivity and optical absorption in terms of the pseudogap. This model was used to describe the fluctuation region of quasi-one-dimensional systems that undergo a Peierls transition,[7] with the result that the predictions of this model are in good quantitative agreement with optical experiments on KCP and TTF-TCNQ,[8] at least at sufficiently high temperatures.

A form of this model was considered in Ref. 9 as an extension[7] to the fluctuation region of a commensurable Peierls transition. The exact solution[6,7] was obtained in the limit of large range of the close-order correlation, and qualitative criteria were indicated for the applicability of this treatment for a finite correlation

length. In the present paper an exact solution for the one-electron Green's function is obtained in the form of a continued fraction, and also for the density of electron states, for arbitrary values of the correlation length for shortrange order; this permits us to trace a smooth transition to the "metallic" state (pseudogap filled in) as the correlation length is decreased and to justify the qualitative criteria given earlier[7] for the use of the asymptotic form for large correlation lengths.

1. FORMULATION OF THE MODEL AND ANALYSIS OF THE FEYNMAN DIAGRAMS

We consider an electron in a Gaussian random field $\Delta(x)$ with the correlation function

$$\langle \Delta(x)\Delta(x') \rangle = \Delta^2 \exp[-|x-x'|\xi^{-1}]\cos 2p_F(x-x'), \qquad (1)$$

where Δ^2 gives the mean square fluctuation of the field, ξ is the correlation length (close-order correlation range), and p_F in the Fermi momentum of the electrons. This is precisely the correlator that is obtained for the fluctuations of the order parameter in the one-dimensional Ginzburg-Landau model for the Peierls transition,[10] and therefore we shall speak of it in concrete terms as a Peierls system in the fluctuation region.

It must be noted that our assumption that the random field $\Delta(x)$ is Gaussian obviously does not apply to real Peierls systems, at least for sufficiently low temperatures $T \ll T_{p0}$, where T_{p0} is the temperature of the Peierls transition in the self-consistent field approximation.[11] We are considering the Gaussian model of a Peierls system [with the exact correlator (1)] because it admits of an exact solution, derived below, and also because it is evidently not so very far from reality in the region $T \sim T_{p0}$.

The correlation length will be regarded as a parameter of the theory, just as the quantity Δ^2 is. Finding them requires a complete microscopic theory of the Peierls transition. The model under consideration can also be derived in a certain variant of the static approximation of the dynamic theory of the Peierls transition,[6,9] (the assumption that there is a clearly expressed

central peak in the dynamic structure factor of the lattice which is undergoing the Peierls transition). The model can also have a bearing on the properties of liquid semiconductors.[6]

The Fourier transform of (1) (the static structure factor) is of the form

$$S(Q) = 2\Delta^2 \left\{ \frac{\varkappa}{(Q-2p_F)^2+\varkappa^2} + \frac{\varkappa}{(Q+2p_F)^2+\varkappa^2} \right\}, \tag{2}$$

where $\varkappa = \xi^{-1}$. The simplest proper-energy part of the one-electron Green's function is given by (p is the momentum of the electron)

$$\Sigma(\varepsilon_n p) = \Delta^2 \int \frac{dQ}{2\pi} S(Q) \frac{1}{i\varepsilon_n - \xi_{p+q}}, \tag{3}$$

and is shown graphically in Fig. 1, a, where the wavy line corresponds to the formula (2) and the solid line is the free Green's function of the electron. Here ξ_p is the energy of free electrons, measured from the Fermi level, and $\varepsilon_n = (2n+1)\pi T$.

We shall deal in the most detail with the case of almost free electrons:

$$\xi_p = p^2/2m - \mu \approx v_F(|p|-p_F), \tag{4}$$

where m is the mass of the electron, v_F is the Fermi velocity, and μ is the chemical potential. Furthermore $2p_F$ is in general considered to be incommensurable with the period of the initial lattice.

Besides this, we shall consider the selected[9] case of the spectrum in the strong coupling approximation

$$\xi_p = -W \cos pa, \tag{5}$$

where a is the initial lattice period, setting $2p_F = \pi/a$, which corresponds to a half-filled band with doubled period, i.e., to the case of limiting commensurability, when the Peierls order parameter becomes real.

From Eqs. (2) and (3) we get (we shall consider the initial momentum of the electron $p_\infty + p_F$)

$$\Sigma(\varepsilon_n p) = \Delta^2 \{i\varepsilon_n + \xi_p + iv_F\varkappa\}^{-1}$$
$$= \Delta^2 G_0(\varepsilon_n, -\xi_p - iv_F\varkappa), \tag{6}$$

where we have used the fact that for a one-dimensional system $\xi_{p-2p_F} = -\xi_p$. The expression (6), which corresponds to the simplest diagram, Fig. 1, a, was taken as the basis of the analysis conducted in the paper of Lee, Rice, and Anderson.[10] In Refs. 6 and 7 all diagrams of the Gaussian model of the Peierls transition were summed in the asymptotic case $\varkappa \to 0$, which, as can be seen from Eq. (6), is justified when the inequality

$$v_F\varkappa = v_F\xi^{-1} \ll \xi_p; 2\pi T \tag{7}$$

is satisfied. This imposes a limitation on the description of the immediate neighborhood of the Fermi level.
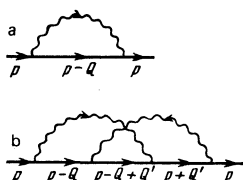
FIG. 1.

Our problem is now to sum all of the graphs of the Gaussian model for finite $\varkappa$.

As was stated earlier,[7] in each order of perturbation theory the contribution of one order is given by diagrams with a sequence of successive vertices with incoming or outgoing interaction lines transmitting a momentum $Q \sim \pm 2p_F$. Diagrams of the type of Fig. 1, b are small of the order of the parameter ξ_p/ε_F (ε_F is the Fermi energy), and can be dropped. Therefore in order $2n$ ($2n$ is the number of vertices) we need include only $n!$ diagrams. Figure 2 shows all essential diagrams of sixth order. Let us consider the contribution of the diagram 2, d. After elementary calculations we find that the quantity corresponding to Fig. 2, d is

$$\Delta^6 \frac{1}{i\varepsilon_n-\xi_p} \frac{1}{i\varepsilon_n+\xi_p+iv_F\varkappa} \frac{1}{i\varepsilon_n-\xi_p+2iv_F\varkappa} \frac{1}{i\varepsilon_n+\xi_p+3iv_F\varkappa}$$
$$\times \frac{1}{i\varepsilon_n-\xi_p+2iv_F\varkappa} \frac{1}{i\varepsilon_n+\xi_p+iv_F\varkappa} \frac{1}{i\varepsilon_n-\xi_p}.$$

The contributions for the other diagrams of Fig. 2 are entirely analogous; the numbers over the electron lines in Fig. 2 indicate how many times $iv_F\varkappa$ occurs in the corresponding denominator. We note that the contribution of the "crossed" diagram Fig. 2, d is equal to that of the diagram without crossing of the interaction lines, Fig. 2, e. We emphasize that the simplicity of the expressions for the contributions of the various diagrams is due to the choice of the structure factor $S(Q)$ in the Lorentzian form (2).

In eighth order there are in all $4! = 24$ essential diagrams; all of the irreducible diagrams are shown in Fig. 3. The corresponding contributions are easily found and are analogous in form, and the use of the numbers over the electron lines is as in Fig. 3. Furthermore, again there are quite a number of equalities among the diagrams: $a = b = c = d$; $e = f = g = h$; $i = j$; $k = l$.

The general rules for writing out the expression corresponding to an arbitrary diagram are now clear. The contribution of any diagram is determined by the arrangement of the initial and final vertices (in Fig. 3 they are marked with the letters I and F). In each electron line following a vertex of type I a term $iv_F\varkappa$ is added in the denominator, and in an electron line fol-
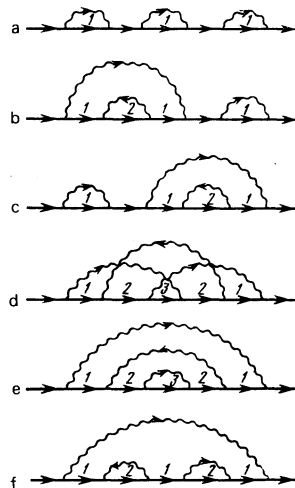
FIG. 2.
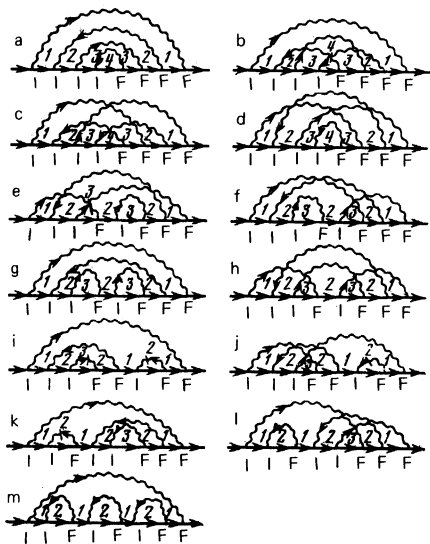
FIG. 3.

lowing a vertex of type F, such a term is subtracted. In this connection, the sense (direction) of the interaction lines is immaterial.

These rules hold also for the treatment of the problem with spectrum (5) in the strong-coupling approximation for the half-filled band. Here, however, we must include also diagrams of the type of Fig. 1, b, in which the interaction lines do not have to be arranged in succession according to the directions of motion of the transferred momentum, since with the spectrum (5) the points $p, p + 2p_F$, and $p - 2p_F$ are equivalent (with $2p_F = \pi/a$),[9] i.e., all possible diagrams. Then in order $2n$ there are in all $(2n - 1)!! = (2n - 1)!/2^{n-1}(n - 1)!$ diagrams, and also the contribution of each interaction line is multiplied by 2.[9] The rule about the appearance of terms $iv_F \varkappa$ in denominators of Green's functions is the same as before.

We then follow a method proposed (for a different problem) by Elyutin.[13] From the foregoing it is easy to see that the contribution of any diagram is determined by the arrangement of initial and final vertices. Furthermore any diagram with intersecting interaction lines can be uniquely represented by a diagram without any intersections, since any diagram with intersections is equivalent to some diagram without any. The recipe for the construction of the corresponding diagram without intersections (for a given arrangement of I and F vertices) is: Counting from the left, the first final vertex must be connected with an interaction line to the nearest initial vertex on its left, and so on for the remaining vertices not so far connected with interaction lines. Thus, for example, the diagrams of Fig. 3, b, c, d reduce to the form of Fig. 3, a, the diagrams Fig. 3, e, f reduce to the form of Fig. 3, g, and so on. For a fixed distribution of initial vertices in a problem with the electron spectrum (4) the final vertices can be chosen only from points of opposite parity, but for a problem with the spectrum (5) the final vertices can be chosen also from points of the same parity as the initial ones. The numbers put with the electron lines in Figs. 2 and 3 can be transferred to the vertices, by

assigning to a vertex the number of terms $iv_F \varkappa$ in the denominator corresponding to the line proceeding after that vertex. The general rule is[13]: To an initial vertex is assigned the number $N_n = N_{n-1} + 1$, where N_{n-1} is the number assigned to the nearest vertex on the left. To a final vertex is assigned the number $N_n - 1$. Also $N_0 = 0$, and n is the order number of a vertex.

Let us introduce

$$v(k) = \begin{cases} (k+1)/2 & k = 2m+1 \\ k/2 & k = 2m \end{cases} \tag{8}$$

for a problem with the spectrum (4) and

$$v(k) = k \tag{9}$$

for a problem with the spectrum (5). Then it can be verified that the number of irreducible self-energy diagrams which are equal to a given diagram without intersections of interaction lines is equal to the product of the quantities $v(N_n)$ for all initial vertices of that diagram.[13] Accordingly, we can conduct all further arguments in terms of diagrams without intersections of interaction lines by applying to all initial vertices the appropriate factors $v(N_m)$.

2. THE ONE-ELECTRON GREEN'S FUNCTION

Any diagram for an irreducible proper-energy part, when restructured according to the rules that have been formulated here, contains an all-surrounding interaction line, i.e., reduces to the form shown in Fig. 4, a. This enables us to derive recurrence formulas for determining a proper-energy part, which are the basis of Elyutin's method.[13] By the definition of a proper-energy part, we have the Dyson equation for the Green's function:

$$G^{-1}(\varepsilon_n \xi_p) = G_0^{-1}(\varepsilon_n \xi_p) - \Sigma_1(\varepsilon_n \xi_p), \tag{10}$$

where (see Fig. 4, a)

$$\Sigma_1(\varepsilon_n \xi_p) = \frac{\Delta^2}{(i\varepsilon_n + \xi_p + iv_F \varkappa)^2} \Xi_1(\varepsilon_n \xi_p) = \Delta^2 G_0^{-2}(\varepsilon_n, -\xi_p - iv_F \varkappa) \Xi_1(\varepsilon_n \xi_p), \tag{11}$$

and for $\Xi_1(\varepsilon_n \xi_p)$ we have the expansion of Fig. 4, b in terms of diagrams without intersections of interaction lines, with the factors $v(N_n)$ applied to their vertices. This expansion can be expressed in the standard way in terms of the corresponding irreducible graphs:

$$\Xi_1(\varepsilon_n \xi_p) = G_0^{-2}(\varepsilon_n, -\xi_p - iv_F \varkappa) \{ G^{-1}(\varepsilon_n, -\xi_p - iv_F \varkappa) - \Sigma_2(\varepsilon_n \xi_p) \}, \tag{12}$$

where $\Sigma_2(\varepsilon_n \xi_p)$ can be expressed as a sum of the ir-
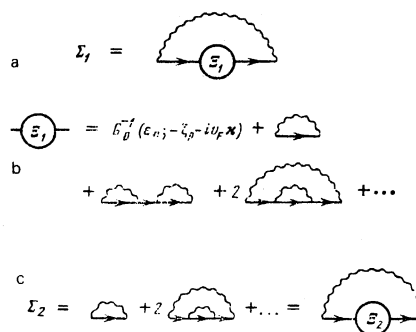
FIG. 4.

reducible graphs of Fig. 4, c:

$$\Sigma_2(\varepsilon_n\xi_p) = \Delta^2 G_0^2(\varepsilon_n, \xi_p - 2iv_F\varkappa)\Xi_2(\varepsilon_n\xi_p), \quad (13)$$

$$\Xi_2(\varepsilon_n\xi_p) = G_0^{-2}(\varepsilon_n, \xi_p - 2iv_F\varkappa)\{G_0^{-1}(\varepsilon_n, \xi_p - 2iv_F\varkappa) - \Sigma_3(\varepsilon_n\xi_p)\} \quad (14)$$

and so on. We have finally:

$$\Sigma_k(\varepsilon_n\xi_p) = \Delta^2 G_0^2(\varepsilon_n, (-1)^k\xi_p - ikv_F\varkappa)v(k)\Xi_k(\varepsilon_n\xi_p), \quad (15)$$

$$\Xi_k(\varepsilon_n\xi_p) = G_0^{-2}(\varepsilon_n, (-1)^k\xi_p - ikv_F\varkappa)\{G_0^{-1}(\varepsilon_n, (-1)^k\xi_p - ikv_F\varkappa) - \Sigma_{k+1}(\varepsilon_n\xi_p)\}, \quad (16)$$

$$\Sigma_k(\varepsilon_n\xi_p) = \frac{\Delta^2 v(k)}{G_0^{-1}(\varepsilon_n, (-1)^k\xi_p - ikv_F\varkappa) - \Sigma_{k+1}(\varepsilon_n\xi_p)}. \quad (17)$$

This is the fundamental recurrence formula. The Green's function is accordingly expressible in the form of a continued fraction:

$$G(\varepsilon_n\xi_p)$$
$$= \cfrac{1}{i\varepsilon_n - \xi_p - \cfrac{\Delta^2}{i\varepsilon_n + \xi_p + iv_F\varkappa - \cfrac{\Delta^2}{i\varepsilon_n - \xi_p + 2iv_F\varkappa - \cfrac{2\Delta^2}{i\varepsilon_n + \xi_p + 3iv_F\varkappa - \cdots}}}}$$
$$\equiv \left[0; \frac{1}{i\varepsilon_n - \xi_p}, \frac{-\Delta^2}{i\varepsilon_n + \xi_p + iv_F\varkappa}, \ldots, \frac{-\Delta^2 v(k)}{i\varepsilon_n - (-1)^k\xi_p + ikv_F\varkappa}, \ldots\right].$$
$$(18)$$

For $\varkappa = 0$ we can use the well known representation of the incomplete Γ function as a continued fraction[14]:

$$\Gamma(a, x) = \int_x^\infty dt\, e^{-t}t^{a-1} = \cfrac{x^a e^{-x}}{x + \cfrac{1-a}{1 + \cfrac{1}{x + \cfrac{2-a}{1+\cdots}}}}, \quad (19)$$

and also the relation $\Gamma(0, x) = -Ei(-x)$ to verify that

$$G(\varepsilon\xi_p)_{\varkappa=0} = \frac{\varepsilon + \xi_p}{\Delta^2}\exp\left(-\frac{\varepsilon^2 - \xi_p^2}{\Delta^2}\right)Ei\left(\frac{\varepsilon^2 - \xi_p^2}{\Delta^2}\right)$$
$$= \int_0^\infty d\zeta\, e^{-\zeta}\frac{\varepsilon + \xi_p}{\varepsilon^2 - \xi_p^2 - \zeta\Delta^2} = \int_0^\infty dW\, P_R(W)\frac{\varepsilon + \xi_p}{\varepsilon^2 - \xi_p^2 - W^2}, \quad (20)$$

where the usual analytic continuation $i\varepsilon_n \to \varepsilon \pm i\delta$ is to be understood. Here

$$P_R(W) = \frac{2W}{\Delta^2}\exp\left(-\frac{W^2}{\Delta^2}\right) \quad (21)$$

is the Rayleigh distribution[15] which describes the uniform fluctuations of a semiconducting slit over all space. The Rayleigh distribution arises because in this case we have to do with a complex Gaussian field of fluctuations.[15] Accordingly, for $\varkappa = 0$ we get the result of Ref. 6. In the general case ($\varkappa \neq 0$) we cannot put the expression (18) in any closed form, but the continued-fraction representation is convenient for numerical computation.

For the problem with the spectrum (5) and $2p_F = \pi/a$ (limiting commensurable case, doubled period) we get in a similar way the recurrence relation (17) with $v(k)$ given by Eq. (9), so that

$$G(\varepsilon_n\xi_p)$$
$$= \cfrac{1}{i\varepsilon_n - \xi_p - \cfrac{2\Delta^2}{i\varepsilon_n + \xi_p + iv_F\varkappa - \cfrac{2\cdot 2\Delta^2}{i\varepsilon_n - \xi_p + 2iv_F\varkappa - \cfrac{3\cdot 2\Delta^2}{i\varepsilon_n + \xi_p + 3iv_F\varkappa - \cdots}}}}$$
$$= \left[0; \frac{1}{i\varepsilon_n - \xi_p}, \frac{-2\Delta^2}{i\varepsilon_n + \xi_p + iv_F\varkappa}, \ldots, \frac{-k\cdot 2\Delta^2}{i\varepsilon_n - (-1)^k\xi_p + ikv_F\varkappa}, \ldots\right].$$
$$(22)$$

Here Δ^2 has a coefficient 2 owing to the necessity of including the two directions of interaction lines, as explained earlier.

For $\varkappa = 0$ we can again use Eq. (19), and after simple calculations we get

$$G(\varepsilon\xi_p)_{\varkappa=0} = -\frac{1}{2\Delta}\left(\frac{\xi_p+\varepsilon}{\xi_p-\varepsilon}\right)^{1/2}\exp\left(-\frac{\varepsilon^2-\xi_p^2}{4\Delta^2}\right)\Gamma\left(\frac{1}{2}, -\frac{\varepsilon^2-\xi_p^2}{4\Delta^2}\right)$$
$$= \frac{1}{\pi^{1/2}}\int_0^\infty d\zeta\exp\left(-\frac{\zeta^2}{4}\right)\frac{\varepsilon+\xi_p}{\varepsilon^2-\xi_p^2-\zeta^2\Delta^2} = \int_{-\infty}^\infty dW\, P_G(W)\frac{\varepsilon+\xi_p}{\varepsilon^2-\xi_p^2-W^2},$$

where (23)

$$P_G(W) = \frac{1}{2\pi^{1/2}\Delta}\exp\left(-\frac{W^2}{4\Delta^2}\right), \quad (24)$$

which agrees with the result obtained in Ref. 9. The appearance of the Gaussian distribution here is due to the fact that in this case we are dealing with a real Gaussian field of fluctuations. In the general case, $\varkappa \neq 0$, we are also obliged to use the continued-fraction representation (22) for the Green's function.

3. THE DENSITY OF STATES

Let us proceed to the calculation of the density of electron states corresponding to the Green's functions (17) and (22). For the problem with the spectrum (4) (incommensurable transition) we have

$$\frac{N(\varepsilon)}{N_0} = -\frac{1}{\pi}\int_{-\infty}^\infty d\xi_p\,\mathrm{Im}\,G^R(\varepsilon\xi_p)$$
$$= -\frac{1}{\pi}\int_{-\infty}^\infty d\xi_p\frac{\mathrm{Im}\,\Sigma_1(\varepsilon\xi_p)}{[\varepsilon-\xi_p-\mathrm{Re}\,\Sigma_1(\varepsilon\xi_p)]^2 + \mathrm{Im}^2\Sigma_1(\varepsilon\xi_p)}, \quad (25)$$

where N_0 is the density of states of free electrons at the Fermi level. From the fundamental recurrence relation (17) we have:

$$\mathrm{Re}\,\Sigma_k(\varepsilon\xi_p) = \frac{\Delta^2 v(k)[\varepsilon-(-1)^k\xi_p-\mathrm{Re}\,\Sigma_{k+1}(\varepsilon\xi_p)]}{[\varepsilon-(-1)^k\xi_p-\mathrm{Re}\,\Sigma_{k+1}(\varepsilon\xi_p)]^2 + [kv_F\varkappa-\mathrm{Im}\,\Sigma_{k+1}(\varepsilon\xi_p)]^2},$$
$$(26)$$
$$\mathrm{Im}\,\Sigma_k(\varepsilon\xi_p) = \frac{-\Delta^2 v(k)[kv_F\varkappa-\mathrm{Im}\,\Sigma_{k+1}(\varepsilon\xi_p)]}{[\varepsilon-(-1)^k\xi_p-\mathrm{Re}\,\Sigma_{k+1}(\varepsilon\xi_p)]^2 + [kv_F\varkappa-\mathrm{Im}\,\Sigma_{k+1}(\varepsilon\xi_p)]^2}.$$

Calculations of the density of states were made with a BÉSM-6 computer; the convergence of the iteration procedure (26) was found to be very good. The results are shown in Fig. 5, where the different curves of the density of states correspond to different values of the dimensionless parameter $\Gamma = v_F\varkappa/\Delta = v_F\xi^{-1}/\Delta$. The curve with $\Gamma = 0$ corresponds to the case in which the density of states can be found analytically.[7] It can be seen that as the correlation length ξ decreases there is a gradual filling up of the pseudogap, i.e., a transition to a "metallic" state. For $v_F\xi^{-1} \ll \Delta$ the approximation $\varkappa = 0$ works very well everywhere except in the range
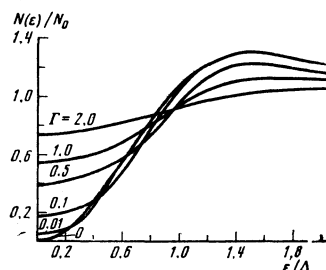
FIG. 5.

of energies $\sim v_F \xi^{-1}$ around the Fermi level, which confirms the qualitative conclusions of previous papers.[6,7] For large values $\Gamma \gtrsim 2$ the difference between the results of Lee, Rice, and Anderson,[10] based on the use of only the one diagram of Fig. 1, a, and those of the present calculation done by including all graphs becomes inappreciable. The main difference appears for small Γ, when the approach of Ref. 10 predicts a transition to a density of states of the BCS type for $\Gamma \to 0$.

Figure 6 shows the dependence of the density of states on the Fermi level (which governs, for example, the Pauli paramagnetic susceptibility) as a function of Γ. Curve 1 is our result, and curve 2 is the result of Ref. 10 (adjusted to our notation). It can be seen that the filling in of the pseudogap occurs more rapidly in our model; for $\Gamma < 1.5$ curve 1 can be approximated with the formula $N(0)/N_0 \approx (0.541 \pm 0.013)\Gamma^{1/2}$.

In attempts to compare our results with experiments on the Peierls transition in KCP or TTF-TCNQ it must be kept in mind that we have neglected all nongaussian fluctuations, which may be important for $T \ll T_{p0}$.[11] This Gaussian model can be applied for $T \lesssim T_{p0}$, or for KCP and TTF-TCNQ for $T \gtrsim 200$ K at any rate. From neutron diffraction and x-ray data it follows[16,17] that at these temperatures in KCP $\xi > 10^2 a$ (a is the lattice constant), i.e., $\Gamma \propto \varepsilon_F a/\Delta \xi < 0.1$, which may explain the good agreement of the results obtained in Refs. 6 and 7 for the optical absorption by the pseudogap with experiments on KCP (Ref. 18, see also Ref. 8). There is no generally accepted theory of the correlation length for the Peierls transition. The experimental data do not contradict the results of Blunck,[19] which indicate that $\xi(300$ K$) \gtrsim 10^2 a$, $\xi(200$ K$) \gtrsim 10^3 a$, i.e., $\Gamma(300$ K$) \lesssim 0.1$, $\Gamma(200$ K$) \lesssim 0.01$. The nongaussian character of the fluctuations for $T \ll T_{p0}$ evidently leads to a more sharply expressed pseudogap in the density of states,[11] which can also be seen in the optical experiment.[18] We note, however, that in the range of temperatures when a sharper gap is observed experimentally, evidently three-dimensional ordering effects are already important.

For the extreme case of commensurability [the spectrum (5)] we have

$$\frac{N(\varepsilon, W)}{N_0} = -\frac{1}{\pi} \int_{-W}^{W} \frac{d\xi_p}{(1-\xi_p^2/W^2)^{1/2}} \frac{\mathrm{Im}\,\Sigma_i(\varepsilon\xi_p)}{[\varepsilon-\xi_p-\mathrm{Re}\,\Sigma_i(\varepsilon\xi_p)]^2+\mathrm{Im}^2\Sigma_i(\varepsilon\xi_p)}.$$

(27)

The iteration procedure is given by the formulas (26) with the substitution $k \to 2k$. Figure 7 shows the results of calculations of the density of states for the case $W \to \infty$ (infinitely broad band) which is most simply
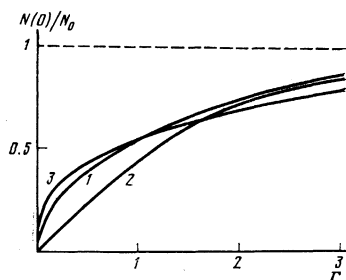
FIG. 6.
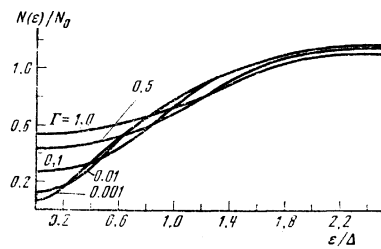
FIG. 7.

compared with the free electron case which we have considered. For finite values of W there is a characteristic peak of the density of states at $\varepsilon = W$,[9] owing to the smearing out of the singularity at the edge of the band of the one-dimensional metal. Furthermore, in the case $W \gg \Delta$ the form of the density of states for $\varepsilon \lesssim \Delta$ is practically not different from that obtained in the limit $W \to \infty$, and this is precisely the region of most interest to us. Again it can be seen that as ξ decreases there is a smooth transition to a metallic state. The density of states at the Fermi level as a function of Γ is shown for this problem as curve 3 in Fig. 6.

Again it is easy to trace the transition to the case 0, for which the problem can be solved analytically[9]; this approximation works well when the inequalities (7) are satisfied. For $\Gamma < 3$ curve 3 is approximated by the formula $(0.546 \pm 0.016)\Gamma^{1/3}$. There is a curious coincidence in the values of the constants in the expressions for the density of states at the Fermi level as function of the parameter Γ in the two different problems. In the case now being considered (commensurable) the pseudogap in the density of states is less sharply expressed, and it is filled in much more rapidly as ξ decreases, than in the incommensurable case previously considered, and the criterion for the applicability of the approximation $\Gamma = 0$ is more strictly quantitative in this case, although qualitatively it is again expressed by the inequalities (7).

In conclusion the writer expresses his deep gratitude to B. M. Letfulov for carrying out the numerical calculations. He is also grateful to S. A. Brazovskii and L. V. Keldysh for discussions and for their interest in this work.

[1]B. I. Halperin, Adv. Chem. Phys. 13, 123 (1968).

[2]V. L. Berezinskii, Zh. Eksp. Teor. Fiz. 65, 1251 (1973) [Sov. Phys. JETP 38, 620 (1974)].

[3]A. A. Abrikosov and I. A. Ryzhkin, Adv. Phys. 27, 147 (1978).

[4]A. A. Ovchinnikov and N. S. Erikhman, Zh. Eksp. Teor. Fiz. 73, 650 (1977) [Sov. Phys. JETP 46, 340 (1977)].

[5]A. A. Abrikosov, L. P. Gor'kov, and I. E. Dzyaloshinskii, Metody kvantovoi teorii polya v statisticheskoi fiziki (Methods of quantum field theory in statistical physics), Fizmatgiz, 1963. English transl., New York, Prentice-Hall, 1963.

[6]M. V. Sadovskii, Zh. Eksp. Teor. Fiz. 66, 1720 (1974) [Sov. Phys. JETP 39, 845 (1974)].

[7]M. V. Sadovskii, Fiz. Tverd. Tela 16, 2504 (1974) [Sov. Phys. Solid State 16, 1632 (1975)].

[8]W. Wonneberger, J. Phys. C 10, 1073 (1977).

[9]W. Wonneberger and R. Lautenschlager, J. Phys. C 9, 2865 (1976).

[10]P. A. Lee, T. M. Rice, and P. W. Anderson, Phys. Rev. Lett. 31, 462 (1973).

[11]S. A. Brazovskii and I. E. Dzyaloshinskii, Zh. Eksp. Teor.

Fiz. **71**, 2338 (1976) [Sov. Phys. JETP **44**, 1233 (1976)].

[12]M. V. Sadovskiĭ, Preprint FIAN (Fiz. Inst. Akad. Nauk) No. 63, 1973.

[13]P. V. Elyutin, Opt. Spektrosk. **43**, 542 (1977) [Opt. Spectrosc. (USSR) **43**, 318 (1977).

[14]Bateman Manuscript Project, A. Erdelyi, Ed., Higher Transcendental functions, Vol. 2, New York, McGraw-Hill, 1953.

[15]S. M. Rytov, Vvedenie v statisticheskuyu radiofiziku (Introduction to Radio Physics), Nauka, 1966.

[16]R. Comès, M. Lambert, H. Launois, and H. R. Zeller, Phys. Rev. **B8**, 571 (1973).

[17]J. W. Lynn, M. Iizumi, G. Shirane, S. A. Werner, and R. B. Saillant, Phys. Rev. **B12**, 219 (1975).

[18]P. Bruesch, S. Strassler, and H. R. Zeller, Phys. Rev. **B12**, 1154 (1975).

[19]M. Blunck, Phys. Lett. **62A**, 237 (1978); Z. Phys. **B31**, 1 (1978).

Translated by W. H. Furry

Instability of cholesteric liquid crystals in an electric field

V. G. Chigrinov, V. V. Belyaev, S. V. Belyaev, and M. F. Grebenkin

Research Institute for Organic Intermediate Products and Dyes
(Submitted 25 May 1979)
Zh. Eksp. Teor. Fiz. **77**, 2081–2092 (November 1979)

The field instability threshold (U_c) and the deformation period (T_c) have been calculated for four Grandjean bands (the layer thickness L of the cholesteric liquid crystal (CLC) was comparable with the helix pitch p_0) by numerical integration, starting out from the general equations of continual theory of CLC. The calculations were made in the case of initial planar and twist orientations of the director of the CLC at the substrate for domains with different directions. For Grandjean bands with large numbers ($L \gg p_0$) analytic formulas are proposed for the calculation of T_c and U_c with account of the nonequilibrium pitch of the cholesteric helix. Detailed experimental investigation of the instability threshold and the deformation period for the cases mentioned above have shown excellent agreement of experimental results and theoretical calculations.

PACS numbers: 61.30.Gd

1. INTRODUCTION

A field (zero-current) instability is observed in the planar texture of a cholesteric liquid crystal (CLC) with positive dielectric anisotropy ($\Delta\varepsilon = \varepsilon_\| - \varepsilon_\perp > 0$) at some threshold voltage U_c upon application of an electric field parallel to the helix axis. This instability appears in the form of a spatially periodic deformation of the initial orientation of the director of the liquid crystal and is due to the destabilizing moment, which is proportional to $E^2\Delta\varepsilon^1$ (E is the intensity of the electric field). In nematic liquid crystals (NLC) the threshold voltage of the analogous instability (Freedericsz transition[1]) is determined by the formula

$$U_F = 2\pi(\pi K_{11}/\Delta\varepsilon)^{1/2}, \qquad (1)$$

where K_{11} is the elastic modulus for a transverse flexure deformation; the wave vector of the deformation is equal to zero in this case. For CLC the theoretical value of the threshold U_c and the period of the deformation $T_0 = 2\pi/k$ (k is the wave vector of the deformation) were obtained by Helfrich[2] and refined by Hurault:[3]

$$U_c^2 = \frac{8\pi^3}{\Delta\varepsilon}(6K_{22}K_{33})^{1/2}\frac{L}{p_0}, \qquad (2)$$

$$T_c^2 = \left(\frac{3K_{33}}{2K_{22}}\right)^{1/2}p_0 L; \qquad (3)$$

here L is the thickness of the CLC, p_0 is the equilibrium helical pitch, K_{33} and K_{22} are the elastic moduli for deformations of longitudinal bending and torsional defor-

mations, respectively.

The dependences $U_c \propto (L/p_0)^{1/2}$ and $T_c \propto (p_0 L)^{1/2}$ that follow from (2) and (3) have been verified experimentally.[4,5] Formulas (2) and (3) were obtained, however, under the assumption that $L \gg p_0$ and without account of the difference of the real (induced) helical pitch p, which arises as a result of the orienting influence of the walls of the vessel,[1,6] from the equilibrium value p_0, and therefore cannot be used directly for the estimation of the instability threshold in the case of a thickness of the CLC layer that is comparable with the helical pitch ($L \sim p_0$). In the case $L \sim p_0$, only the electrohydrodynamic instability has been investigated experimentally in detail.[6]

The purpose of the present work is a systematic theoretical and experimental study of the field instability of planar texture of CLC in the case of arbitrary relations between the layer thickness L and the helical pitch p_0, with account of the real pitch and the boundary conditions.

2. THEORETICAL CALCULATION

Theoretical consideration of the field instability in planar texture of CLC has been carried out under the assumption of a rigid connection of the CLC molecules with the surface of the cell at the boundaries of the layer. Two cases are considered: the directions of orientations of the molecules on the boundaries of the surface are parallel (planar orientation) or perpendic-